Applied Nanoscience (2020) 10:3443–3455
https://doi.org/10.1007/s13204-020-01472-1

ORIGINAL ARTICLE

Synthesis and catalytic practicality of CeO_2 nanoparticle: an excellent heterogenous candidate for 4-nitrophenol reduction

Dadu Mal[1] · Aamna Balouch[1,2] · Sirajuddin[3] · Abdullah[1] · Ali Muhammad Mahar[1] · Abdul Hameed Pato[1] · Sagar Kumar[1] · Shanker Lal[1] · Aneel Kumar[1]

Received: 1 March 2020 / Accepted: 30 May 2020 / Published online: 24 June 2020

Abstract
The present study is based on a synthesis of facile, cheaper, well homogenized and highly stable Cerium Oxide nanostructures via chemical precipitation method. The synthesized nanoceria was subjected under different characterization tools. The UV–visible and FTIR study profile initially confirm the formation and existing functionalities in nanoceria. The XRD, SEM techniques were exploited the crystalline and untwined combined form rhombohedron shaped CeO_2 nanoparticles respectively. While zeta sizer measurements explained well arranged, mono-dispersity, size and charge over the surface of nanoceria, which was calculated to be 17 nm with a desirable charge of + 6.37 mV. Finally, the well-prepared nanoceria nanoparticles were successfully applied as effective heterogeneous catalyst for 4-nitrophenol reduction. Under optimized conditions the nanoceria exhibited enhanced activity for 99% reduction of 4-NP within 60 s reaction time under greener microwave irradiation.

Keywords Cerium oxide · Chemical precipitation · 4-nitrophenol

Introduction

Currently, cerium has been paid great attention to the researchers due to its appreciated applications in engineering and technology. Furthermore, Cerium is very reactive with atmospheric oxygen and readily form a metal oxide with varying composition and known as ceria. In bulk, Cerium oxide has two form having different oxidation states (CeO_2 and Ce_2O_3) (Tsai et al. 2008). It is the only rare earth element which shows stable tetravalent oxidation state unlike other members of lanthanide series mainly exist in trivalent oxidation state (Dao et al. 2011). Numerous methods have been attempted for the synthesis of cerium oxide NPs including precipitation (Pelletier et al. 2010), hydrothermal (Rojas et al. 2012; Alhaji et al. 2019), solvothermal (Zhang et al. 2011,2018), ball milling (Yadav and Srivastava 2012), thermal decomposition (Wang et al. 2002), spray pyrolysis (Demokritou et al. 2013), thermal hydrolysis (Hirano et al. 2000), and sol–gel methods (He et al. 2012; Darroudi et al. 2014a,b). Amongst all co-precipitation is most satisfactory, economical, simple and widely used at laboratory scale level (Farahmandjou et al. 2016).Cerium oxide NPs are widely applied for the treatment of several organic pollutants from the environment and aqueous system also (Li et al. 2018). Additionally, it is used for oxygen sensing (Zhao et al. 2017), pharmacological agent (Celardo et al. 2011), dye degradation (Li et al. 2018), medicines (Shcherbakov et al. 2020), catalysis (Pato et al. 2019; Mahar et al. 2020), fuel oxidation catalysis (Jung et al. 2005), and automotive exhaust treatment (Campbell and Peden 2005). Currently, water pollution is caused by various nitroarenes compounds due to vast usage in different industries such as pesticides, explosives and dyes (Zhang et al. 2018). The conversion of nitroarenes into anilines received much significance because of wide applications in numerous pharmaceutical and dyestuff products (Budanov et al. 2010). Industrial and agricultural activities nitro-phenolic compounds found to be a major pollutant

✉ Aamna Balouch
aamna_balouch@yahoo.com

1 National Centre of Excellence in Analytical Chemistry, University of Sindh, Jamshoro 76080, Pakistan

2 Department of Physics Engineering, Faculty of Science and Letters, Istanbul Technical University, Maslak, 34469 Istanbul, Turkey

3 International Centre for Chemical and Biological Sciences, HEJ Research Institute of Chemistry, University of Karachi, Karachi 75270, Pakistan

in the aquatic system (Aditya et al. (2015)). The US Environmental Protection Agency (EPA) has listed 4-NP as major toxicant due to hazardous effect as it may damage liver, kidneys and central nervous system in humans and animals (Guo et al. 2014; Feng et al. 2009). Many harmful chemicals are produced on daily basis due to rapid development of various industries i.e. Fertilizers, dyes, pharmaceuticals and textile etc. (Feng et al. 2009; Saravanakkumar et al. 2019; Vincent and Guibal 2004; Deka et al. 2014). The reduction of 4-NP yields 4-AP which is pharmaceutically important candidate and being utilized as intermediate for the synthesis of a vast number of antipyretic and analgesic drugs like paracetamol, phenacetin (Chinnappan et al. 2016). Unfortunately, 4-NP is organic refractory toxicant which severely affects the environment indulging the ecosystem including aquatic animals as well as humans and consequently results in several lethal diseases (Bordbar et al. 2018). Under mild environmental conditions, Sodium borohydride is applied as a reductant/initiator for the reduction of 4-NP to 4-AP in aqueous media, which is cheap, simple, and greener one. However, the conversion is very slow in the absence of a suitable catalyst by comparing all reported conversion methods (Kojima et al. 2002; Liu et al. 2009). In addition, different conventional methods have been reported i.e. sonolysis method and Fenton degradation process. In former degradation process, the products formed were NO_2^-, NO_3^-, and H^+ and later degradation practice employment of "Fenton reagent", which is a mixture of a ferrous salt and H_2O_2. In this process, advanced oxidation takes places involving the hydroxyl radical as the oxidation agent (Zhang et al. 2007; Shahwan et al. 2011), but these methods are not very much effective. Therefore, it is more important to find a suitable/convenient ecofriendly and potential catalyst for the direct hydrogenation of 4-NP applying $NaBH_4$ as reductant. Nowadays, the use of nonmaterial as an efficient catalyst has been attracted by researchers because of remarkable electronic properties and high surface to volume ratio. The noble metals like Au (Suchomel et al. 2018), Ag (Mohamed and Al-Sharif 2013), Pt (Pandey and Mishra 2014), and non-noble metals like Cu (Deka et al. 2014), Ni (Yang et al. 2014), Pd (Harish et al. 2009), have widely been used with different morphologies and sizes as a competent catalyst to reduces the 4-NP into 4-AP, which is major contamination in aquatic system. In Aqueous media, 4-NP has a greater stability and low solubility, so it is difficult job to degrade, to resolve water pollution issue numerous semiconductor materials including, TiO_2 (Ahn et al. 2007), ZnO (He et al. 2018), and Cu_2O (Liu et al. 2015) have been reported. Furthermore, different methods have been developed typical chemical catalysis and photocatalysis (Zhao et al. 2017; Magdalane et al. 2019). The catalytic degradation of 4NP to 4-AP utilizing excess $NaBH_4$ as reductant is an important one. Because 4-AP is less hazardous and has huge demand in the industrial application (Liu et al. 2018a). Most of the synthetic protocol for metal nanomaterials is chemical reduction which creates hazardous environmental problems and chemical toxicity. In Environmental remediation photocatalytic process is considered a greener one, which assists to decreases the unwanted generation of by-products at mild experimental conditions and is becoming a fascinating alternative for the reduction of nitroarenes. In this regard, several efforts have been made to find out the ideal conditions for photocatalytic reduction of nitroaromatic compounds into anilines (Hernández-Gordillo et al. 2013; Ramírez-Rave et al. 2015; Guerrero-Araque et al. 2017; Castañeda et al. 2019; Wang et al. 2009; Imamura et al. 2011; Cipagauta et al. 2014).

Scientifically Cerium dioxide has importance in photocatalysis due to excellent physicochemical properties which include, chemical stability, redox capacity, non-toxicity, corrosion protection and Ce^{3+} defects in CeO_{2-x}. At nanoscale, ceria possesses high redox cycling between Ce^{4+}/Ce^{3+} ions in the semiconductor surface which make them a super candidate for photocatalyst (Chang et al. 2016; Li et al. 2017; Channei et al. 2014). The pure cerium oxide (IV) nanomaterial has not been reported for the catalytic reduction of 4-NP to 4-AP so far. Ceria@Y_2O_3 Binary metal oxide NPs was successfully synthesized by hydrothermal approach and applied as a heterogeneous catalyst for selective reduction of 4-NP into 4-AP utilizing an excess of $NaBH_4$ as a reductant. The reduction reaction completed in 4 min and follows pseudo-first-order kinetics (Magdalane et al. 2017). Another approach was made by researchers to fabricate CeO_2@CdO binary metal oxide nanocomposites by simple precipitation and hydrothermal method and tested against gram-negative and gram-positive bacteria along with applied as a heterogeneous photocatalyst for the degradation of toxic Rh-B dye (Magdalane et al. 2016). Various authors have reported their work on ceria as photocatalyst for the degradation of organic species present in wastewater. Khan et al. (2011) have degraded toxic dyes namely amido black and acridine orange by 45.6% and 37.7% respectively with an irradiation time of 170 min using hollow spheres CeO_2 as photocatalyst. Yang et al (2010) published their work using hollow spheres CeO_2 as efficient adsorbent material for the removal of Congo red dye 84% from the wastewater photocatalytically. Enhance photocatalytic degradation of acid orange 7 was observed under visible light irradiation using mesoporous CeO_2 material. The author compares CeO_2 with TiO_2 P25, ceria shows excellent photocatalytic behavior than bulk counterpart (Ji et al. 2008).

This study mainly focuses on the synthesis of cost-effective and eco-friendly nanocatalyst with exceptional photocatalytic properties and excellent reusability towards nitroarene compounds.

Experimental work

Glasswares and chemical reagents

In this experimental study, all the needed glasswares were soaked overnight in (10% v/v) HNO_3 solution to prevent from any contamination and then rinsed three times with distilled water and dried in an oven at 100 °C before used for the experiment. All chemicals were extra pure and analytical grade used without further purification. The precursor salt cerium ammonium nitrate $(NH_4)_2[Ce(NO_3)_6]$ was purchased from Dae-Jung China, NH_4OH (33%) is used as reducing agent, 4-nitro phenol (4-NP), sodium borohydride ($NaBH_4$), were obtained from Sigma Aldrich, extra pure Milli-Q water was used a solvent throughout the study.

Synthetic procedure for CeO_2 nanocatalyst

The ceria (CeO_2) nanostructures were synthesized by simple co-precipitation method at room temperature using 0.548 g (0.01 M) of $(NH_4)_2[Ce(NO_3)_6]$ as a precursor salt in 250 mL two neck round bottom flask containing 100 mL of milli-Q water then solution was sonicated for 05 min at 28 ± 1 °C for complete homogenation. Then the entire solution was stirred magnetically for 10 min after that 10 mL of NH_4OH (33%) solution as a reducing agent was taken in burette added dropwise ultimately pH of the solution was reached at 10 and resultant color of solution rapidly changes from orange to straw yellow which confirms the formation of particles. The constant vigorous magnetic stirring was carried out for 30 min until complete precipitation was achieved. The precipitate was washed several times with Milli-Q water up to neutral pH then lastly washed with ethanol. After washing, CeO_2 nanostructures were dried in a vacuum oven at 80 °C overnight, then annealed at 400 °C for 3 h.

Heterogeneous catalytic application of CeO_2

In this experimental study, CeO_2 nanostructures have been used as an efficient heterogeneous catalyst for the reduction of 4-NP to 4-AP under low power microwave irradiation in aqueous media. The catalytic reduction of 4-NP was carried out under normal laboratory conditions, 10 mL of 15 μM 4-nitrophenol solution was taken in Pyrex glass tube. The solution was tightly sealed and irradiated with microwave in the presence and absence of catalyst material. During the reaction, the 4-NP solution was continuously monitored and irradiated with constant low power microwave radiation. To check the catalytic performance of CeO_2 nanostructures for 4-NP reduction The UV–Visible spectrophotometer (Biochrom Libra S22) is employed to check the absorption spectrum after every 10 s of reaction interval by taking 3 mL (500 μL of 4NP, 2.5 mL of H_2O and catalyst dose) in quartz crystal cuvette cell (1 cm path length) and the spectrum is recorded.

Conditions for reduction of 4-NP

Appropriate amount of catalyst, 4-NP and $NaBH_4$ were taken in Quartz Crystal cell path length of 1 cm at the normal environmental condition. UV–Visible spectra were recorded following four suitable procedure which includes: (a) constant concentration of 4-NP with variable concentration of reductant ($NaBH_4$) in the absence of catalyst, (b) fixed concentration of reducing agent and 4-nitrophenol utilizing constant microwave power time interval using suitable amount of catalyst, (c) at a constant concentration of 4-NP and $NaBH_4$ with a variable quantity of catalyst, and (d) all the quantities catalyst dose, 4-NP concentration and reducing agent $NaBH_4$ were optimized and the solution mixture was irradiated with low power microwave. For better results, it was found that CeO_2 nanostructure (100 μg) and Reducing agent (0.0005 M) and low power microwave irradiation for 60 s were suitable for complete reduction of 4-NP to 4-AP. During the experimental study the % reduction was calculated from the change in absorption profile of 4-NP using the given equation:

$$\frac{C_{i-}C_f}{C_f} \times 100.$$

Herein, C_i is the initial concentration of 4-nitrophenol and C_f is the final concentration respectively.

Characterization

Different analytical techniques were performed to characterize the cerium oxide nanoparticles. The UV–Visible study was carried out in the range of 200–800 nm with a scan rate of 2 nm (Biochrom Libra S22). FT-IR (Thermo Nicolet 5700) study was performed to investigate the functionality of material from 400 to 4000 cm^{-1}. The crystalline phase and purity of the sample were checked employing X-ray diffraction (Bruker D8 Model) with CuKα radiation. The size distribution and surface potential of synthesize material were investigated by employing zeta sizer-potential technique while the size and surface morphology were disclosed by SEM (JSM 6380 of Joel, Japan).

Results and discussion

SEM analysis

To check the surface topography of engineered cerium oxide nanoparticle SEM analysis was carried out. This

study reveals that the material has untwined combined form rhombohedron shaped morphology as shown in Fig. 1a, b. The low magnification image shows agglomerated rhombohedron shaped particles. In high-resolution SEM images reveals homogenized well separated untwined combined form rhombohedron shaped CeO_2 nanoparticles with a particle size in the range of 18–20 nm. The sharp aged shape of particles proved as efficient photocatalyst in for organic contamination.

X-ray diffraction study

The freshly prepared powdered nanoceria sample was explored through XRD technique. The crystallinity and phase purity of the material was investigated using X-ray diffraction (Bruker D8 Model) with CuKα irradiation and scanning rate of $0.025°s^{-1}$. It can be seen from the diffraction plane at 110, 200, 220, 311, 222, 400, 331, 420 which confirms the cubic phase nature of the material (Majeed et al. 2019). Nonappearance of impurity indicates that pure CeO_2 is synthesized by the chemical precipitation method and shows the good agreement with JCPDS No 34-0394. Furthermore, the Debye Scherrer formula was used to calculate the average crystalline size of the engineered CeO_2 NPs using the most intense plane in the diffractogram, a formula is given below (Truffault et al. 2010):

$$\tau = \frac{K\lambda}{\beta \cos\theta}.$$

Here τ is the mean crystalline size K is the dimensionless form factor taken as a constant which has a value of 0.9, lambda (λ) is the wavelength of the incident X-rays radiation, β (FWHM) which represents the width at the mean peak height and θ is the diffraction angle (Fig. 2). Average size of pure nanoceria was coming in nanometric range and calculated theoretically using the above-given equation and found to be 18 ± 2 nm.

Zeta sizer and potential study

This study was exploited to know the size distribution of synthesized material using Zeta Sizer (Zetasizer Ver. 7.11 MALVAREN). Fresh powdered Ceria sample was prepared by taking 3 mg of sample into the water, thoroughly dispersed placed in vial then analyzed through zeta sizer different peaks were observed within the range of 100 nm the average size of CeO_2 nanomaterial was found to be 50 ± 5 nm. After that the same sample was analyzed to check the surface charge of the material because zeta sizer has

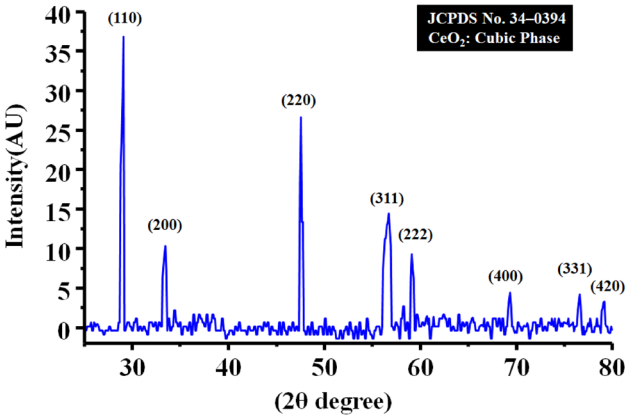

Fig. 2 XRD pattern of the CeO_2

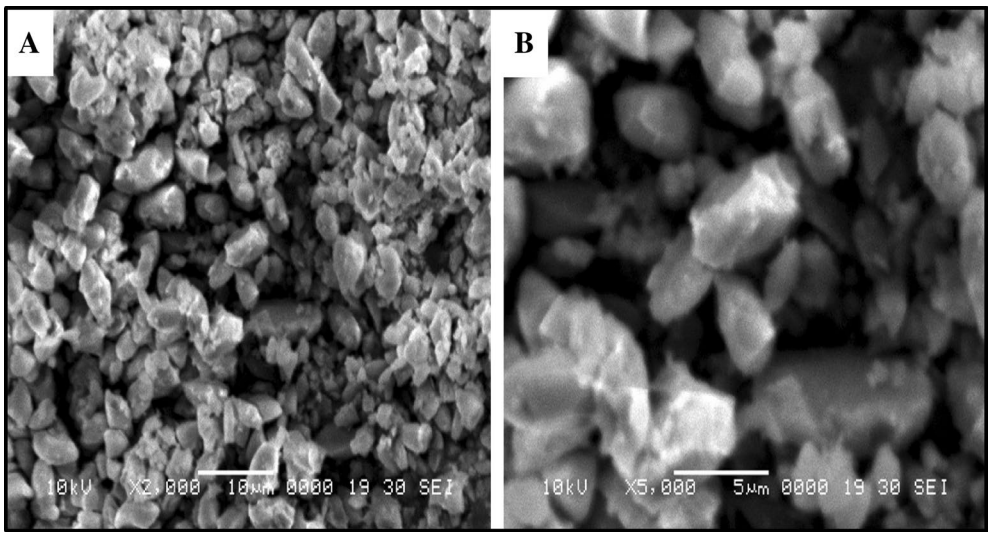

Fig. 1 SEM images of CeO_2 nanostructures **a** low resolution and **b** high resolution

another mode known as zeta potential which is used to calculate the surface potential of particles and ceria has surface potential charge of + 6.37 mV which exhibit good catalytic applicability (Fig. 3).

FT-IR study

To check the surface functionality of cerium oxide nanomaterial FT-IR study was performed in the range of 4000–400 cm^{-1} (Fig. 4). The broad absorption band at 3443 cm^{-1} confirms the OH stretching vibration which displays absorption of water on the surface of the material (Majeed et al. 2019; Anand et al. 2019), another band at 1600 cm^{-1} shows N–H stretching mode of vibration, the peak at 1400 cm^{-1} exhibit C–H bending along with the appearance of the small band at 1000 cm^{-1} is due C–O stretching it might be due to environmental CO_2 and major absorption band around 540 cm^{-1} it confirms Ce–O stretching vibration (Rajendran et al. 2014; Santos et al. 2008).

UV–Visible study

To check the synthesized material basic characterization techniques were performed. The synthesize material was confirmed through UV–Visible spectroscopy a very common technique was employed in the range of 200–600 nm in range. CeO_2 nanoparticle shows a maximum absorption in the Ultraviolet range and maximum lambda max was observed at 322 nm (Calvache-Muñoz et al. 2017), which is shown in Fig. 5a. Along with the UV–Visible peak stability study was carried out to monitor the stability the synthesized cerium oxide NPs is highly stable up to 2 month as depicted in Fig. 5b.

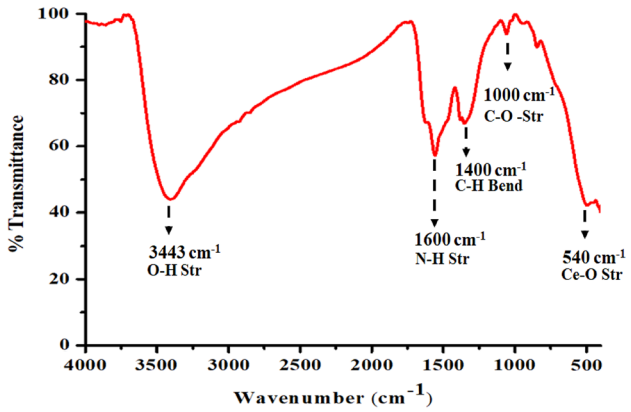

Fig. 4 (FT-IR) Fourier transform Infrared investigation of CeO_2 nanostructures

The catalytic applicability of CeO_2 nanostructures

The catalytic performance of CeO_2 nanostructures was monitored for the reduction of 4-NP using microwave irradiation. The UV–Visible absorption study was carried out from 200–800 nm range. The UV–Visible absorption spectrum of 4-nitrophenol (15 µM) solution shows major characteristics peaks at 318 nm shown in Fig. 6a. The peak at 318 nm corresponding to the 4-nitrophenol molecule, when a small quantity of reducing agent was added a small change in spectral profile of 4-NP was observed due to formation of 4-nitrophenolate ion and absorption is shifted to longer wavelength approximately 400 nm resultant changes in color was observed from light yellow to bright yellow which is depicted in Fig. 6b. Heterogeneous catalytic applicability of CeO_2 NPs toward 4-NP was evaluated from a decrease in absorption of 4-nitrophenolate ion at 400 nm and ultimately the appearance of small peak around 300 nm confirms the

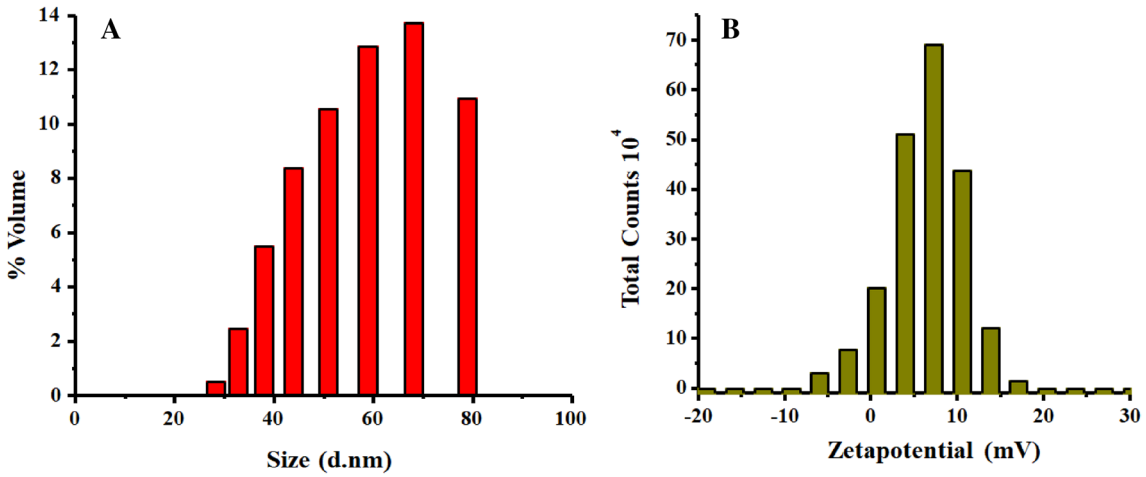

Fig. 3 Zeta sizer profile (**a**) and Zeta potential profile (**b**) of CeO_2 nanocatalyst

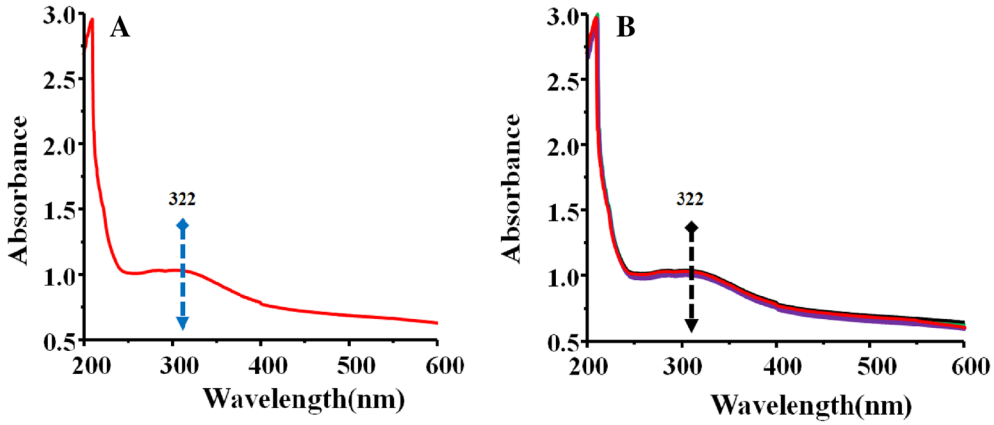

Fig. 5 **a** UV–Visible absorption profile. **b** Stability of nanocatalyst

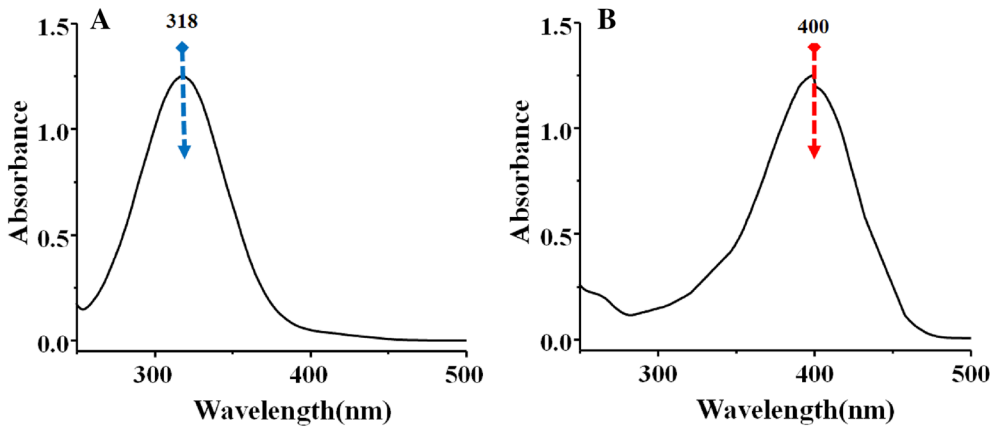

Fig. 6 **a** UV–Visible spectra of 4-NP (15 µM) solution. **b** Absorption profile of 4-nitrophenolate ion solution

formation of 4-AP (He et al. 2014), from reduction mechanism using greener source of energy microwave irradiation.

Effect of reducing agent

The 4-NP with a concentration of 15 µM was used during experimental study. The UV–Visible profile of 4-NP shows a maximum absorption at 318 nm which confirms from the reported literature (Shah et al. 2017). When a 2 µL small quantity of reducing agent $NaBH_4$ (0.0005 M) was added into the standard 4NP solution with the same concentration, red shift was observed optical density shifted from 318 nm (black line) to 400 nm (Red line) due to the formation of 4-nitrophenolate ion in the solution and there is no change in peak height was observed in both spectra were given in Fig. 7a. After that, the concentration of $NaBH_4$ was increased but no further shifting to longer or shorter wavelength was observed but peak intensity is decreased slowly. Therefore the effect of reducing agent concentration towards concentration of 4-NP conducted. Herein the dose of $NaBH_4$was optimized at a constant concentration of 4-NP in the absence of a catalyst. To improve % reduction variant amount of reducing agent was used from 5–20 µL with a concentration of 0.0005 M. Initially the 4-NP peak at 400 nm decreased gradually with increasing the amount of $NaBH_4$ Fig. 7(b-c). After achieving 15% reduction in concentration no significant change was noticed therefore 20 µL of $NaBH_4$ was selected as optimized concentration for further study.

Effect of low power microwave radiation

After optimizing $NaBH_4$ concentration, the effect of greener and instant source of energy microwave was exploited. The commercial microwave oven with constant power (110 W) was used in the absence of reducing agent and catalyst material during experimental study. The reduction in the concentration of 4-NP was observed with increasing the time

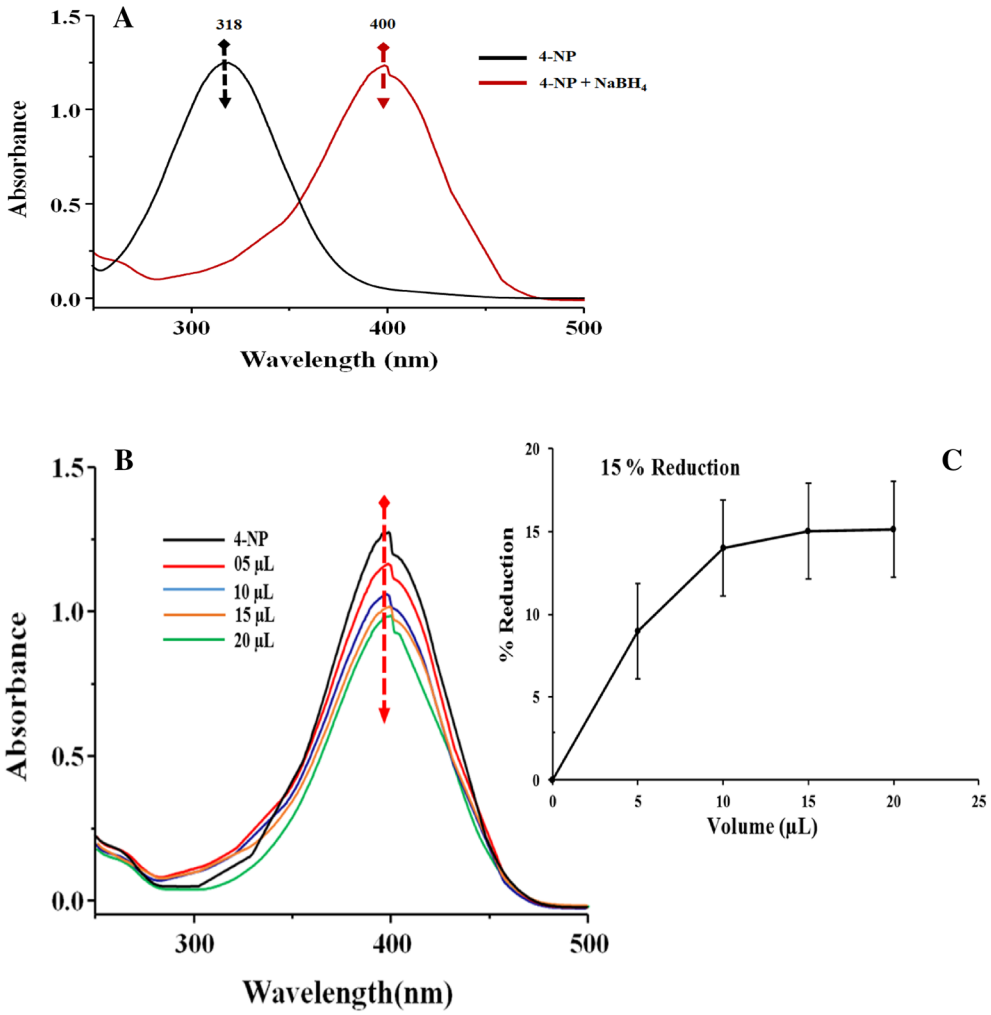

Fig. 7 **a** Spectral changes of 4-nitrophenol solution before (black line) and after (red line) addition of 0.0005 M $NaBH_4$ solution. **b** UV–Visible absorption spectra of 4-nitrophenol (15 µM) solution without catalyst using $NaBH_4$ solution 0.0005 M concentration. **c** % reduction of 4-NP at the different volume of $NaBH_4$

from 10 to 60 s with a 10 s of the interval at constant power (110 W). Total 27.5% reduction in the concentration of 4-NP was attained within 60 s of at constant microwave radiation exposure (Fig. 8).

Effect of catalyst dose

After successful optimization of $NaBH_4$ and microwave radiation with 25% reduction of 4-NP concentration with respect to time the effect of CeO_2 nanocatalyst was checked. After the addition of nanocatalyst a considerable drop in intensity of peak at 400 nm was observed which shows approximately 40% reduction in 4-NP concentration, results has been depict in Fig. 9a. Later on, the catalyst amount was increased from 20 to 120 µg at optimized condition and changes in the absorption profile of 4-nitrophenolate ion, % reduction were calculated. It was confirmed from the absorption profile as the amount of catalyst increase the gradual decrease in peak intensity is obtained. Total 87.74% reduction in 4-NP is obtained at 120 µg within 40 s. Simultaneously a small peak was also observed around 300 nm which is due to the formation of 4-AP. The reduction reaction rate faster with increasing the dose of catalysts, which was contributed to the directly increases in the number of catalytic active sites on the surface of nanoceria. It is confirmed from the spectra by increasing the amount of catalyst more active sites were available to accelerate the breakdown of reducing agent $NaBH_4$ hence promoting the rate of reaction faster (Cai et al. 2017).

Time study

Finally, time study was performed using a constant amount of nanocatalyst 100 µg to get the maximum % reduction at

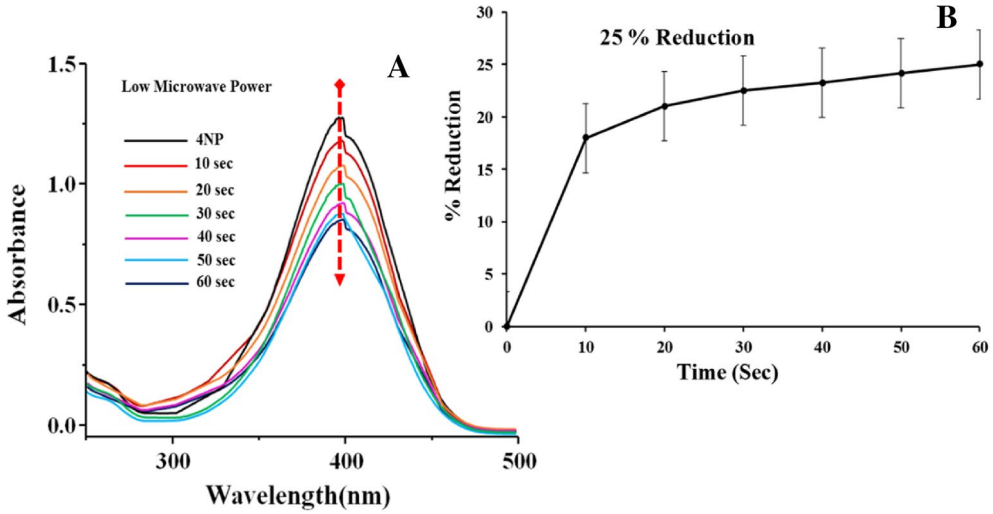

Fig. 8 **a** Optical absorption profile of 15 µM 4-NP solution utilizing constant (110 W) microwave power. **b** % reduction of 4-NP at a different time interval

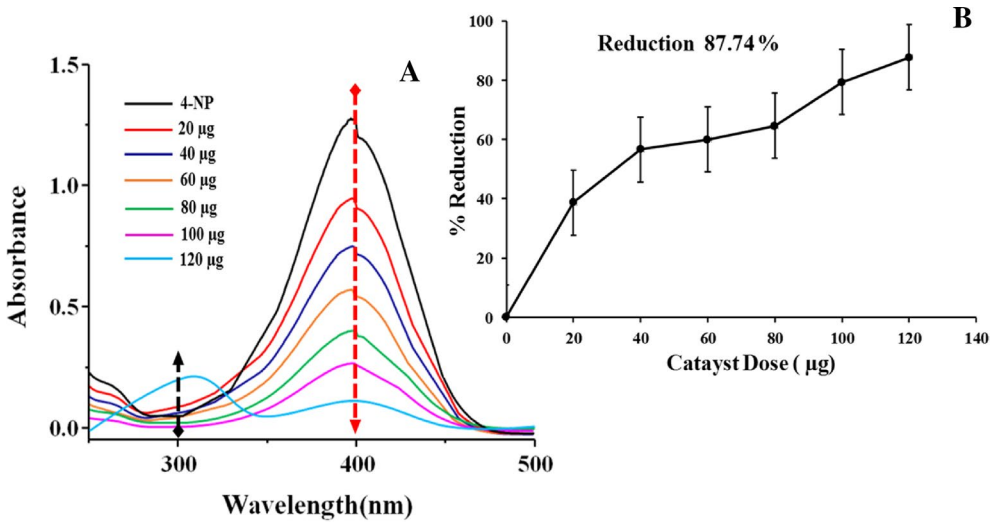

Fig. 9 **a** UV–Visible spectrum of 4-nitrophenol reduction at a different dose of CeO_2 using constant MW and $NaBH_4$. **b** The inset graph shows the 4-nitrophenol % reduction using different amount of nanocatalyst

optimized condition taking $NaBH_4$ 20 µl, low Microwave radiation power 110 W from 10 to 60 s that is depicted in Fig. 10a. It was observed that as the reaction time is enhanced the reduction rate is increased and about 99% decreased in intensity of peak at 400 was achieved within 60 s. The reduction of 4-nitrophenol in the presence of CeO_2 NPs is favorable due to fast hydrogen transfer from $NaBH_4$ under microwave irradiation simultaneously decrease in absorption peak intensity at 400 nm. Appearance of small peak was also observed around 300 nm which is due to formation of 4-aminophenol.

Calibration of 4-nitrophenol

To calculate the unknown amount of 4-NP the standard calibration curve of 4-NP with various concentration was plotted in the range of 1–15 µM at UV–Visible spectrophotometer. Change in absorption peak intensity with respect

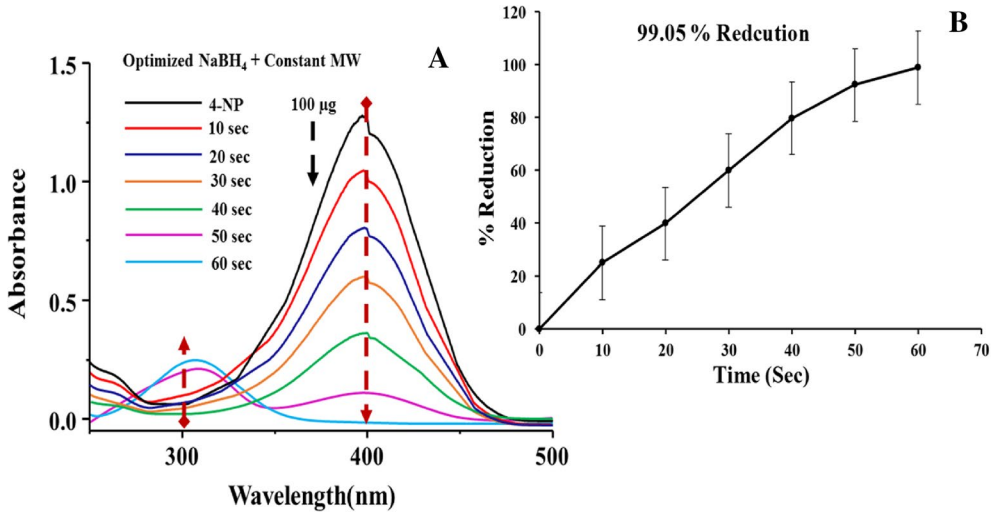

Fig. 10 **a** Optical absorption profile of 4-NP reduction under constant microwave irradiation, optimized $NaBH_4$ and fixed dose of catalyst. **b** % reduction of 4-NP at a different time interval

to the concentration of standard concentration of 4-NP was obtained and standard calibration graph was plotted as per Lambert Beer's Law as shown in Fig. 11a, b. However, the linear regression equation ($y = mx + c$) used for a calibration plot. A straight curve was obtained with a R^2 value of 0.992, $y = 0.1067x + 0.1626$.

Reusability of CeO_2 nanostructure

To check the practical and commercial application of catalyst the reusability of catalyst was performed. The reusability of catalyst plays a great role in socio-economic benefits and environmentally friendly impact of method. Therefore, after the successful catalytic reduction of 4NP, the particles were separated out from the reaction mixture through centrifugation and then filtered with watt man filter paper. The collected material was washed many times with Milli-Q water and dried in an oven under inert condition. The reusability of catalyst was checked, the same particles were applied in the same concentration of the fresh 4-NP solution and the same protocol was followed. To monitor any change in the catalytic performance of ceria nanostructure, five times recycled

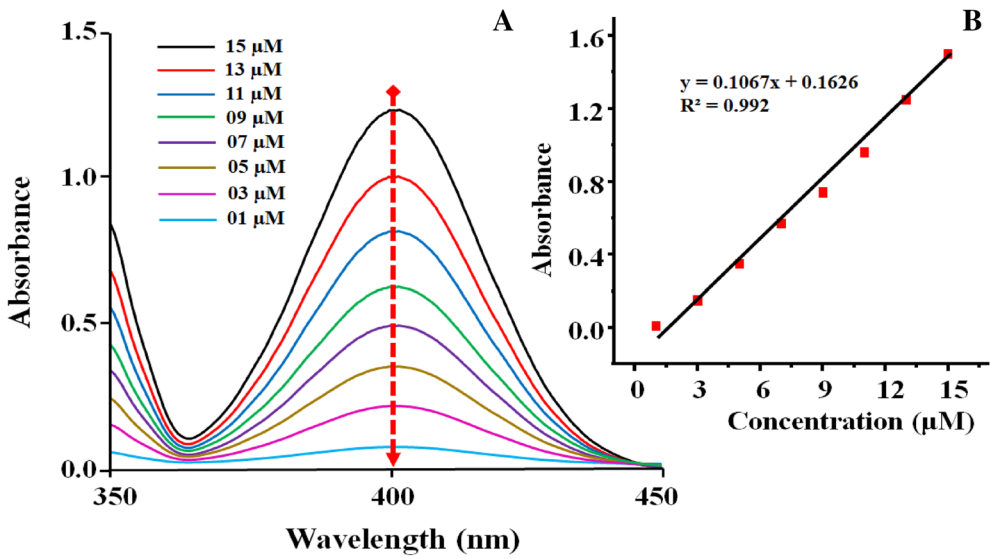

Fig. 11 **a** Standard calibration plot for 4-nitrophenol solutions in the concentration range from 01 to 15 µM. **b** inset showing the corresponding linear calibration plot

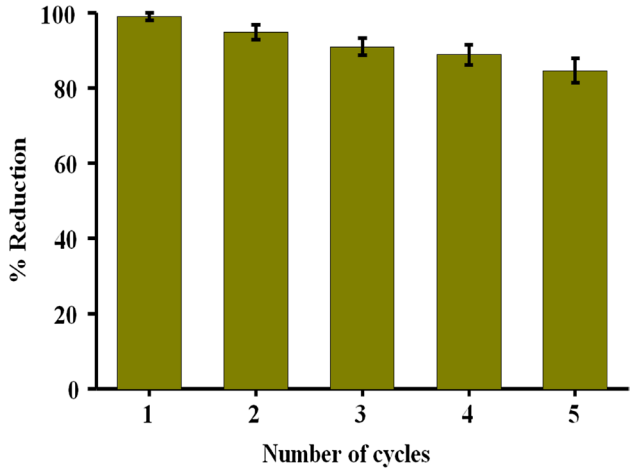

Fig. 12 Reusability study of CeO_2 nanocatalyst for 4-nitrophenol reduction

particles were performed efficiently, and it was observed that catalytic efficiency decreased approximately 8% from 99.05 to 87% as shown in graph Fig. 12. The obtained data indicate the good stability of nanoparticles the decrease in efficiency could be due to the loss of catalyst material during the washing and separation process.

Comparison of CeO_2 nanocatalyst with previously reported literature

At last, we have compared our reported data with already reported methods (Table 1). The comparative study of 4-NP reduction using various heterogeneous nanocatalysts in terms of catalyst dose, reaction time, concentration was conducted. The comparing table shows the present study using CeO_2 NPs as heterogeneous catalyst is cost effective, greener environmentally friendly and far superior then already reported nanocatalyst.

Conclusion

It is concluded that efficient Ceria nanocatalyst was synthesized using ammonium hydroxide as a reducing agent via chemical precipitation which is cheap, facile, lucrative and greener route. The XRD pattern shows that the synthesized material is highly crystalline in nature. The zeta potential data confirms the nanostructured ceria having a highly positive value of + 6.36 mV. The topographical information conducted via SEM analysis which revealed cubic shaped morphology. The enhanced catalytic performance of nanoceria was achieved by the reduction of 4-NP utilizing $NaBH_4$ under microwave radiation. The nanoceria has excellent stability and nanometric size provides a high surface to volume ratio, increased number of active sites and catalytic performance, enabled the proposed nanostructures to get an edge over other materials reported till to date. The outstanding characteristics of cerium oxide make it a phenomenal aspirant for the conversion of 4-nitrophenol into 4-amino phenol.

Table 1 Comparison of reduction efficiency of CeO_2 nanocatalyst over reported candidates used for 4-nitrophenol reduction

Nanocatalyst	Catalyst dose (g)	4-NP Conc: (mM)	% reduction	Time (s)	References
SiO_2/Fe_3O_4	1×10^{-4}	0.02	99.5	240	Shah et al. (2017)
Bi/Fe_3O_4	0.01	10	97	480	Cai et al. (2017)
Au/SiO_2 NPs	0.005	5	98.4	1200	Mehta et al. (2016)
Co NPs	0.003	0.001	90	480	Mondal et al. (2017)
CA-Au and CA-Ag	1.2	0.1	92.2	2700	Saha et al. (2010)
Bentonite clay @Fe NPs	0.01	0.2	96.8	1200	Sravanthi et al. (2019)
Chitosan Guar Gum @Ag	0.0003	2	~75	180	Vanaamudan et al. (2018)
$Co_3O_4/CoFe_2O_4$	0.01	0.2	–	420	Ortiz-Quiñonez and Pal (2019)
Ag NPs-LS hybrid	0.076	0.05	98	360	Liu et al. (2018b)
CeO_2 NPs	1×10^{-4}	0.015	99.05	60	This work

References

Aditya T, Pal A, Pal T (2015) Nitroarene reduction: a trusted model reaction to test nanoparticle catalysts. Chem Commun 51:9410–9431

Ahn W-Y, Sheeley SA, Rajh T, Cropek DM (2007) Photocatalytic reduction of 4-nitrophenol with arginine-modified titanium dioxide nanoparticles. Appl Catal B 74:103–110

Alhaji N, Nathiya D, Kaviyarasu K, Meshram M, Ayeshamariam A (2019) A comparative study of structural and photocatalytic mechanism of $AgGaO_2$ nanocomposites for equilibrium and kinetics evaluation of adsorption parameters. Surf Interfaces 17:100375

Anand T, Renuka D, Ramesh R, Anandaraj L, Sundaram SJ, Ramalingam G, Magdalane CM, Bashir A, Maaza M, Kaviyarasu K (2019) Green synthesis of ZnO nanoparticle using *Prunus dulcis* (Almond Gum) for antimicrobial and supercapacitor applications. Surf Interfaces 17:100376

Bordbar M, Negahdar N, Nasrollahzadeh M (2018) *Melissa Officinalis* L. leaf extract assisted green synthesis of CuO/ZnO nanocomposite for the reduction of 4-nitrophenol and Rhodamine B. Sep Purif Technol 191:295–300

Budanov M, Lefedova O, Ulitin M, Kha NTT (2010) Features of the phenylhydroxylamine catalytic hydrogenation in water solutions of 2-propanole on skeletal nickel. Russ J Phys Chem A 84:1901–1904

Cai K-Y, Liu Y-S, Xu Y, Zhou H, Zhang L, Cui Y (2017) One-pot synthesis of Bi/Fe_3O_4 and its catalytic performances for 4-nitrophenol reduction. Bull Chem React Eng Catal 12:89–95

Calvache-Muñoz J, Prado FA, Rodríguez-Páez JE (2017) Cerium oxide nanoparticles: synthesis, characterization and tentative mechanism of particle formation. Colloids Surf A 529:146–159

Campbell T, Peden CH (2005) Oxygen vacancies and catalysis on ceria surfaces. Science 309:713–714

Castañeda C, Alvarado I, Martínez JJ, Brijaldo MH, Passos FB, Rojas H (2019) Enhanced photocatalytic reduction of 4-nitrophenol over Ir/CeO_2 photocatalysts under UV irradiation. J Chem Technol Biotechnol 94:2630–2639

Celardo I, Pedersen JZ, Traversa E, Ghibelli L (2011) Pharmacological potential of cerium oxide nanoparticles. Nanoscale 3:1411–1420

Chang J, Ma Q, Ma J, Ma H (2016) Synthesis of Fe_3O_4 nanowire@ CeO2/Ag nanocomposites with enhanced photocatalytic activity under sunlight exposure. Ceram Int 42:11827–11837

Channei D, Inceesungvorn B, Wetchakun N, Ukritnukun S, Nattestad A, Chen J, Phanichphant S (2014) Photocatalytic degradation of methyl orange by CeO_2 and Fe–doped CeO_2 films under visible light irradiation. Sci Rep 4:5757

Chinnappan A, Tamboli AH, Chung W-J, Kim H (2016) Green synthesis, characterization and catalytic efficiency of hypercross-linked porous polymeric ionic liquid networks towards 4-nitrophenol reduction. Chem Eng J 285:554–561

Cipagauta S, Hernández-Gordillo A, Gómez R (2014) TiO_2 xerogels prepared by modified sol–gel method with ethylenediamine are photoactive for the 4-nitrophenol photoreduction. J Sol Gel Sci Technol 72:428–434

Dao NN, Dai Luu M, Nguyen QK, Kim BS (2011) UV absorption by cerium oxide nanoparticles/epoxy composite thin films. Adv Nat Sci Nanosci Nanotechnol 2:045013

Darroudi M, Sarani M, Oskuee RK, Zak AK, Hosseini HA, Gholami L (2014a) Green synthesis and evaluation of metabolic activity of starch mediated nanoceria. Ceram Int 40:2041–2045

Darroudi M, Sarani M, Oskuee RK, Zak AK, Amiri MS (2014b) Nanoceria: gum mediated synthesis and in vitro viability assay. Ceram Int 40:2863–2868

Deka P, Deka RC, Bharali P (2014) In situ generated copper nanoparticle catalyzed reduction of 4-nitrophenol. New J Chem 38:1789–1793

Demokritou P, Gass S, Pyrgiotakis G, Cohen JM, Goldsmith W, McKinney W, Frazer D, Ma J, Schwegler-Berry D, Brain J (2013) An in vivo and in vitro toxicological characterisation of realistic nanoscale CeO_2 inhalation exposures. Nanotoxicology 7:1338–1350

Dos Santos M, Lima R, Riccardi C, Tranquilin R, Bueno PR, Varela JA, Longo E (2008) Preparation and characterization of ceria nanospheres by microwave-hydrothermal method. Mater Lett 62:4509–4511

Farahmandjou M, Zarinkamar M, Firoozabadi T (2016) Synthesis of cerium oxide (CeO_2) nanoparticles using simple CO-precipitation method. Revista mexicana de física 62:496–499

Feng ZV, Lyon JL, Croley JS, Crooks RM, Vanden Bout DA, Stevenson KJ (2009) Synthesis and catalytic evaluation of dendrimer-encapsulated Cu nanoparticles. An undergraduate experiment exploring catalytic nanomaterials. J Chem Educ 86:368

Guerrero-Araque D, Acevedo-Peña P, Ramírez-Ortega D, Gómez R (2017) Improving photocatalytic reduction of 4-nitrophenol over ZrO_2–TiO_2 by synergistic interaction between methanol and sulfite ions. New J Chem 41:12655–12663

Guo X, Li X, Jiang Y, Yi L, Wu Q, Chang H, Diao X, Sun Y, Pan X, Zhou N (2014) A spectroscopic study on the interaction between p-nitrophenol and bovine serum albumin. J Lumin 149:353–360

Harish S, Mathiyarasu J, Phani K, Yegnaraman V (2009) Synthesis of conducting polymer supported Pd nanoparticles in aqueous medium and catalytic activity towards 4-nitrophenol reduction. Catal Lett 128:197

He H-W, Wu X-Q, Ren W, Shi P, Yao X, Song Z-T (2012) Synthesis of crystalline cerium dioxide hydrosol by a sol–gel method. Ceram Int 38:S501–S504

He R, Wang Y-C, Wang X, Wang Z, Liu G, Zhou W, Wen L, Li Q, Wang X, Chen X (2014) Facile synthesis of pentacle gold–copper alloy nanocrystals and their plasmonic and catalytic properties. Nat Commun 5:1–10

He L, Tong Z, Wang Z, Chen M, Huang N, Zhang W (2018) Effects of calcination temperature and heating rate on the photocatalytic properties of ZnO prepared by pyrolysis. J Colloid Interface Sci 509:448–456

Hernández-Gordillo A, Romero AG, Tzompantzi F, Oros-Ruiz S, Gómez R (2013) Visible light photocatalytic reduction of 4-nitrophenol using CdS in the presence of Na_2SO_3. J Photochem Photobiol A 257:44–49

Hirano M, Fukuda Y, Iwata H, Hotta Y, Inagaki M (2000) Preparation and spherical agglomeration of crystalline cerium (IV) oxide nanoparticles by thermal hydrolysis. J Am Ceram Soc 83:1287–1289

Imamura K, Iwasaki S-I, Maeda T, Hashimoto K, Ohtani B, Kominami H (2011) Photocatalytic reduction of nitrobenzenes to aminobenzenes in aqueous suspensions of titanium (IV) oxide in the presence of hole scavengers under deaerated and aerated conditions. Phys Chem Chem Phys 13:5114–5119

Ji P, Zhang J, Chen F, Anpo M (2008) Ordered mesoporous CeO_2 synthesized by nanocasting from cubic Ia3d mesoporous MCM-48 silica: formation, characterization and photocatalytic activity. J Phys Chem C 112:17809–17813

Jung H, Kittelson DB, Zachariah MR (2005) The influence of a cerium additive on ultrafine diesel particle emissions and kinetics of oxidation. Combust Flame 142:276–288

Khan SB, Faisal M, Rahman MM, Jamal A (2011) Exploration of CeO_2 nanoparticles as a chemi-sensor and photo-catalyst for environmental applications. Sci Total Environ 409:2987–2992

Kojima Y, Suzuki K-I, Fukumoto K, Sasaki M, Yamamoto T, Kawai Y, Hayashi H (2002) Hydrogen generation using sodium borohydride

solution and metal catalyst coated on metal oxide. Int J Hydrogen Energy 27:1029–1034
Li B, Zhang B, Nie S, Shao L, Hu L (2017) Optimization of plasmon-induced photocatalysis in electrospun Au/CeO_2 hybrid nanofibers for selective oxidation of benzyl alcohol. J Catal 348:256–264
Li S, Hu S, Jiang W, Liu Y, Zhou Y, Liu J, Wang Z (2018) Facile synthesis of cerium oxide nanoparticles decorated flower-like bismuth molybdate for enhanced photocatalytic activity toward organic pollutant degradation. J Colloid Interface Sci 530:171–178
Liu C-H, Chen B-H, Hsueh C-L, Ku J-R, Jeng M-S, Tsau F (2009) Hydrogen generation from hydrolysis of sodium borohydride using Ni–Ru nanocomposite as catalysts. Int J Hydrogen Energy 34:2153–2163
Liu L, Yang W, Sun W, Li Q, Shang JK (2015) Creation of Cu_2O@TiO_2 composite photocatalysts with p–n heterojunctions formed on exposed Cu_2O facets, their energy band alignment study, and their enhanced photocatalytic activity under illumination with visible light. ACS Appl Mater Interfaces 7:1465–1476
Liu Y, Zhang Y, Kou Q, Chen Y, Han D, Wang D, Lu Z, Chen L, Yang J, Xing S (2018a) Eco-friendly seeded Fe_3O_4-Ag nanocrystals: a new type of highly efficient and low cost catalyst for methylene blue reduction. RSC Adv 8:2209–2218
Liu Y, Zhao Y, Zhou Y, Guo X, Chen Z, Zhang W, Zhang Y, Chen J, Wang Z, Sun L (2018b) High-efficient catalytic reduction of 4-nitrophenol based on reusable Ag nanoparticles/graphene-loading loofah sponge hybrid. Nanotechnology 29:315702
Magdalane CM, Kaviyarasu K, Vijaya JJ, Siddhardha B, Jeyaraj B (2016) Photocatalytic activity of binary metal oxide nanocomposites of CeO_2/CdO nanospheres: investigation of optical and antimicrobial activity. J Photochem Photobiol B 163:77–86
Magdalane CM, Kaviyarasu K, Vijaya JJ, Siddhardha B, Jeyaraj B (2017) Facile synthesis of heterostructured cerium oxide/yttrium oxide nanocomposite in UV light induced photocatalytic degradation and catalytic reduction: synergistic effect of antimicrobial studies. J Photochem Photobiol B 173:23–34
Magdalane M, Kaviyarasu K, Arularasu M, Kanimozhi K, Ramalingam G (2019) Structural and morphological properties of Co_3O_4 nanostructures: investigation of low temperature oxidation for photocatalytic application for waste water treatment. Surf Interfaces 17:100369
Mahar M, Balouch A, Talpur FN, Panah P, Kumar R, Kumar A, Pato AH, Mal D, Kumar S, Umar AA (2020) Fabrication of Pt-Pd@ITO grown heterogeneous nanocatalyst as efficient remediator for toxic methyl parathion in aqueous media. Environ Sci Pollut Res 1–9
Majeed HJ, Eftekhari M, Gheibi M, Chamsaz M (2019) Synthesis and application of cerium oxide nanoparticles for preconcentration of trace levels of copper in water and foods followed by flame atomic absorption spectrometry. J Food Meas Charact 13:339–346
Mehta A, Sharma M, Kumar A, Basu S (2016) Gold nanoparticles grafted mesoporous silica: a highly efficient and recyclable heterogeneous catalyst for reduction of 4-nitrophenol. NANO 11:1650104
Mohamed MM, Al-Sharif MS (2013) Visible light assisted reduction of 4-nitrophenol to 4-aminophenol on Ag/TiO_2 photocatalysts synthesized by hybrid templates. Appl Catal B 142:432–441
Mondal A, Mondal A, Adhikary B, Mukherjee DK (2017) Cobalt nanoparticles as reusable catalysts for reduction of 4-nitrophenol under mild conditions. Bull Mater Sci 40:321–328
Ortiz-Quiñonez J-L, Pal U (2019) Borohydride-assisted surface activation of Co_3O_4/$CoFe_2O_4$ composite and its catalytic activity for 4-nitrophenol reduction. ACS Omega 4:10129–10139
Pandey S, Mishra SB (2014) Catalytic reduction of *p*-nitrophenol by using platinum nanoparticles stabilised by guar gum. Carbohydr Polym 113:525–531
Pato H, Balouch A, Talpur FN, Mahar AM, Shah MT, Kumar A, Qasim S, Gabole AA (2019) Synthesis and catalytic practicality of titania@ITO-grown nanoflakes: an excellent candidate for isopropanol conversion to acetone. Appl Nanosci 10(3):739–749
Pelletier DA, Suresh AK, Holton GA, McKeown CK, Wang W, Gu B, Mortensen NP, Allison DP, Joy DC, Allison MR (2010) Effects of engineered cerium oxide nanoparticles on bacterial growth and viability. Appl Environ Microbiol 76:7981–7989
Rajendran R, Shrestha LK, Minami K, Subramanian M, Jayavel R, Ariga K (2014) Dimensionally integrated nanoarchitectonics for a novel composite from 0D, 1D, and 2D nanomaterials: RGO/CNT/CeO_2 ternary nanocomposites with electrochemical performance. J Mater Chem A 2:18480–18487
Ramírez-Rave S, Hernández-Gordillo A, Calderón HA, Galano A, García-Mendoza C, Gómez R (2015) Synthesis of new ZnS–Bipy based hybrid organic–inorganic materials for photocatalytic reduction of 4-nitrophenol. New J Chem 39:2188–2194
Rojas S, Gispert JD, Abad S, Buaki-Sogo M, Victor VM, Garcia H, Herance JRL (2012) In vivo biodistribution of amino-functionalized ceria nanoparticles in rats using positron emission tomography. Mol Pharm 9:3543–3550
Saha S, Pal A, Kundu S, Basu S, Pal T (2010) Photochemical green synthesis of calcium-alginate-stabilized Ag and Au nanoparticles and their catalytic application to 4-nitrophenol reduction. Langmuir 26:2885–2893
Saravanakkumar D, Oualid HA, Brahmi Y, Ayeshamariam A, Karunanaithy M, Saleem AM, Kaviyarasu K, Sivaranjani S, Jayachandran M (2019) Synthesis and characterization of CuO/ZnO/CNTs thin films on copper substrate and its photocatalytic applications. OpenNano 4:100025
Shah MT, Balouch A, Pathan AA, Mahar AM, Sabir S, Khattak R, Umar AA (2017) SiO_2 caped Fe_3O_4 nanostructures as an active heterogeneous catalyst for 4-nitrophenol reduction. Microsyst Technol 23:5745–5758
Shahwan T, Sirriah SA, Nairat M, Boyacı E, Eroğlu AE, Scott TB, Hallam KR (2011) Green synthesis of iron nanoparticles and their application as a Fenton-like catalyst for the degradation of aqueous cationic and anionic dyes. Chem Eng J 172:258–266
Shcherbakov AB, Zholobak NM, Ivanov VK (2020) Biological, biomedical and pharmaceutical applications of cerium oxide. In: Cerium oxide (CeO_2): synthesis, properties and applications. Elsevier, pp 279–358
Sravanthi K, Ayodhya D, Swamy PY (2019) Green synthesis, characterization and catalytic activity of 4-nitrophenol reduction and formation of benzimidazoles using bentonite supported zero valent iron nanoparticles. Mater Sci Energy Technol 2:298–307
Suchomel P, Kvitek L, Prucek R, Panacek A, Halder A, Vajda S, Zboril R (2018) Simple size-controlled synthesis of Au nanoparticles and their size-dependent catalytic activity. Sci Rep 8:1–11
Truffault L, Ta M-T, Devers T, Konstantinov K, Harel V, Simmonard C, Andreazza C, Nevirkovets IP, Pineau A, Veron O (2010) Application of nanostructured Ca doped CeO_2 for ultraviolet filtration. Mater Res Bull 45:527–535
Tsai Y-Y, Oca-Cossio J, Lin S-M, Woan K, Yu P-C, Sigmund W (2008) Reactive oxygen species scavenging properties of ZrO_2–CeO_2 solid solution nanoparticles
Vanaamudan A, Sadhu M, Pamidimukkala P (2018) Chitosan-Guar gum blend silver nanoparticle bionanocomposite with potential for catalytic degradation of dyes and catalytic reduction of nitrophenol. J Mol Liq 271:202–208
Vincent T, Guibal E (2004) Chitosan-supported palladium catalyst. 5. Nitrophenol degradation using palladium supported on hollow chitosan fibers. Environ Sci Technol 38:4233–4240
Wang Y, Mori T, Li JG, Ikegami T (2002) Low-temperature synthesis of praseodymium-doped ceria nanopowders. J Am Ceram Soc 85:3105–3107
Wang H, Yan J, Chang W, Zhang Z (2009) Practical synthesis of aromatic amines by photocatalytic reduction of aromatic nitro compounds on nanoparticles N-doped TiO2. Catal Commun 10:989–994
Yadav T, Srivastava O (2012) Synthesis of nanocrystalline cerium oxide by high energy ball milling. Ceram Int 38:5783–5789

Yang Z, Wei J, Yang H, Liu L, Liang H, Yang Y (2010) Mesoporous CeO_2 hollow spheres prepared by Ostwald ripening and their environmental applications. Eur J Inorg Chem 2010:3354–3359

Yang Y, Zhang Y, Sun CJ, Li X, Zhang W, Ma X, Ren Y, Zhang X (2014) Heterobimetallic metal-organic framework as a precursor to prepare a nickel/nanoporous carbon composite catalyst for 4-nitrophenol reduction. ChemCatChem 6:3084–3090

Zhang H, Fei C, Zhang D, Tang F (2007) Degradation of 4-nitrophenol in aqueous medium by electro-Fenton method. J Hazard Mater 145:227–232

Zhang H, He X, Zhang Z, Zhang P, Li Y, Ma Y, Kuang Y, Zhao Y, Chai Z (2011) Nano-CeO_2 exhibits adverse effects at environmental relevant concentrations. Environ Sci Technol 45:3725–3730

Zhang X-F, Zhu X-Y, Feng J-J, Wang A-J (2018) Solvothermal synthesis of N-doped graphene supported PtCo nanodendrites with highly catalytic activity for 4-nitrophenol reduction. Appl Surf Sci 428:798–808

Zhao X, Wang Y, Feng W, Lei H, Li J (2017) Preparation of Cu(ii) porphyrin–TiO_2 composite in one-pot method and research on photocatalytic property. RSC Adv 7:52738–52746